HYDROLOGICAL PROCESSES
Hydrol. Process. (2010)
Published online in Wiley Online Library
(wileyonlinelibrary.com) DOI: 10.1002/hyp.7888

Estimating flash flood discharge in an ungauged mountain catchment with 2D hydraulic models and dendrogeomorphic palaeostage indicators

J. A. Ballesteros Cánovas,[1]* M. Eguibar,[2] J. M. Bodoque,[3] A. Díez-Herrero,[4] M. Stoffel[5] and I. Gutiérrez-Pérez[6]

[1] *Department of Research and Geoscientific Prospective, Geological Survey of Spain (IGME), Ríos Rosas 23, Madrid E-28003, Spain*
[2] *Department of Hydraulic Engineering and Environment, Institute for Water and Environmental Engineering (IIAMA), Technical University of Valencia, Camino de Vera s/n, Valencia, E-46022, Spain*
[3] *Mining and Geological Engineering Department, University of Castilla-La Mancha, Campus Fábrica de Armas, Avda. Carlos III, Toledo E-45071, Spain*
[4] *Department of Research and Geoscientific Prospective, Geological Survey of Spain (IGME), Ríos Rosas 23, Madrid E-28003, Spain*
[5] *Laboratory of Dendrogeomorphology, Institute of Geological Sciences, University of Berne, CH-3012 Berne, Switzerland Chair for Climatic Change and Climate Impacts, Institute for Environmental Sciences, University of Geneva, CH-1227 Carouge-Geneva, Switzerland*
[6] *Ferrovial-Agromán, Ribera del Loira 42, Madrid, E-28042, Spain*

Abstract:

There is still wide uncertainty about past flash-flood processes in mountain regions owing to the lack of systematic databases on former events. This paper presents a methodology to reconstruct peak discharge of flash floods and illustrates a case in an ungauged catchment in the Spanish Central System. The use of dendrogeomorphic evidence (i.e. scars on trees) together with the combined use of a two-dimensional (2D) numerical hydraulic model and a terrestrial laser scan (TLS) has allowed estimation of peak discharge of a recent flash flood. The size and height distribution of scars observed in the field have been used to define three hypothetical scenarios (S_{min} or minimum scenario; S_{med} or medium scenario; and S_{max} or maximum scenario), thus illustrating the uncertainty involved in peak-discharge estimation of flash floods in ungauged torrents.

All scars analysed with dendrogeomorphic techniques stem from a large flash flood which took place on 17 December 1997. On the basis of the scenarios, peak discharge is estimated to 79 ± 14 m^3 s^{-1}. The average deviation obtained between flood stage and expected scar height was $-0{\cdot}09 \pm 0{\cdot}53$ m. From the data, it becomes obvious that the geomorphic position of trees is the main factor controlling deviation rate. In this sense, scars with minimum deviation were located on trees growing in exposed locations, especially on unruffled bedrock where the model predicts higher specific kinetic energy. The approach used in this study demonstrates the potential of tree-ring analysis in palaeohydrology and for flood-risk assessment in catchments with vulnerable goods and infrastructure. Copyright © 2010 John Wiley & Sons, Ltd.

KEY WORDS palaeoflood; tree rings; TLS; peak discharge estimation; Spanish Central System

Received 26 April 2010; Accepted 2 September 2010

INTRODUCTION

Flash floods are a fast flooding of water often combined with debris transport that usually takes place in high-gradient streams (Jarrett, 1990; Borga *et al*., 2007), but the process may also occur in other settings where sediment is transported easily by heavy rainfalls (Mintegui *et al*., 2006). Flash floods are especially common in mountainous areas where rapid snowmelt or heavy rainfalls are quickly transformed into runoff. Their practically instantaneous occurrence, together with their high capacity of transport, renders flash floods which is one of the most significant weather-related hazards in many parts of the world, causing considerable economic and human losses in each year (Scheuren *et al*., 2008; Gaume *et al*., 2009). The characterization of flash floods with low probability of occurrence and high damage (Merz *et al*., 2009) is crucial, when countermeasures have to be defined in order to minimize associated risks (Enzel *et al*., 1993).

Precipitation records and flow data have been widely used for flood studies (Chow, 1959; Chiang and Chang, 2009); however, the use of systematic data on flash floods presents several challenges in mountainous catchments as representative instrumental records are not normally available in these environments (Benito and Thorndycraft, 2004). In this regard, the use of non-systematic data may improve knowledge of frequency–magnitude relationships of flash floods in ungauged catchmwwents (Baker, 2008).

Historical records (Cook, 1987; Payrastre *et al*., 2005) and sedimentological deposits (Benito *et al*., 2009; Livingston *et al*., 2009) have been successfully used to extend flow time series by hundreds or even thousands of years. However, in mountainous catchments, older palaeoflood deposits are only rarely present because of the high energies prevailing in these high-gradient streams. In addition, documentary records on past events or historical

* Correspondence to: J. A. Ballesteros Cánovas, Department of Research and Geoscientific Prospective, Geological Survey of Spain (IGME), Ríos Rosas 23, Madrid E-28003, Spain. E-mail: ja.ballesteros@igme.es

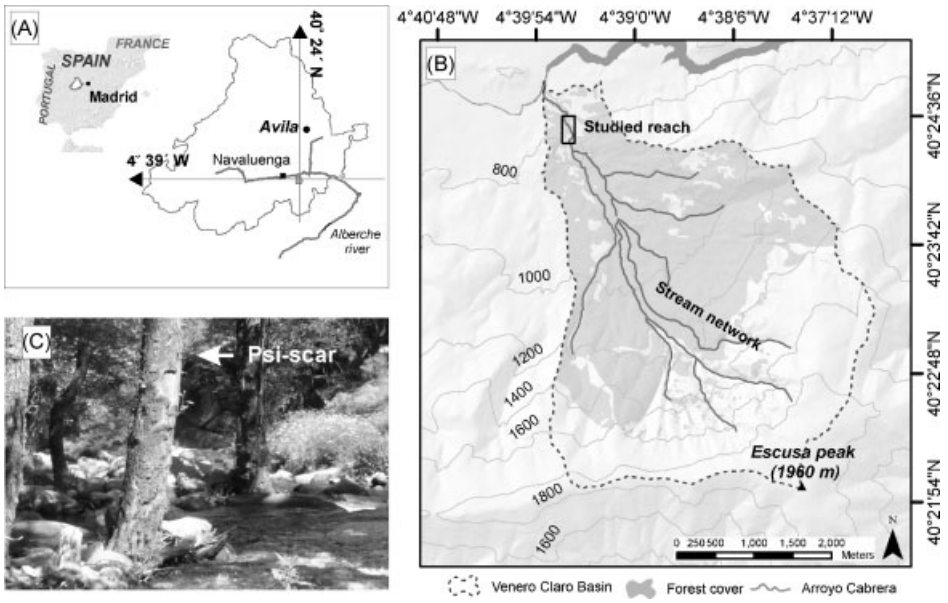

Figure 1. (A) The Arroyo Cabrera is located in the Sierra del Valle near the village of Navaluenga (Ávila), Spanish Central System. (B) Location of the study reach on a schematic map of the Cabrera basin. (C) Scars on trees caused by flash floods in the study area

data are not readily available as these areas were normally only sparsely populated in the past.

Other sources of non-systematic data can be derived from dendrogeomorphic analyses (Alestalo, 1971; Stoffel *et al*., 2010). Scars on trunks, which stem from the impact of debris and wood transported during a flash flood, represent the most common dendrogeomorphic evidence (Yanosky and Jarret, 2002) of past flood activity and can be used as palaeostage indicators (PSI; Baker *et al*., 2002; Jarrett and England, 2002). They are of prime value for the reconstruction of flood frequency (Harrison and Reid, 1967; Gottesfeld and Gottesfeld, 1990; Zielonka *et al*., 2008; Ruiz-Villanueva *et al*., 2010) and help the estimation of flood magnitude. However, the size of past events has been less frequently studied with dendrogeomorphic approaches in the past (Stoffel, 2010).

Previous research on magnitude–frequency relationships of flash floods using tree scars was conducted by Egginton and Day (1977) in low-gradient streams. Later, Gottesfeld (1996) studied the relationship between scar height and adjacent high water marks (HWMs). In addition to the development of different hydraulic methods to estimate peak discharge from PSI or information on HWM (O'Connor and Webb, 1988; Corriell, 2002; Webb and Jarrett, 2002) used 1D computations based on Manning's equation to (i) estimate the stage of past flood events with scars being considered minimum flood-stage indicators and (ii) to reconstruct a recurrence-interval diagram. Nevertheless, despite the potential of PSI from trees for palaeoflood studies (St. George and Nielsen, 2003), knowledge on magnitude reconstructions is still scarce and results have not been validated with outputs from hydraulic models so far.

Therefore, the main objective of this study was (i) to present a methodological approach for realistic peak discharge estimation of flash-flood event with PSI derived from scars on trees and (ii) to apply this methodology to estimate peak discharge of a flash flood which took place on 17 December 1997 in an ungauged catchment of the Spanish Central System. To this end, we (i) used a coupled 2D hydraulic model running on a detailed topography obtained from terrestrial laser scan (TLS) and (ii) defined three hypothetical flood stage scenarios based on scar-size and scar-height distribution so as to reduce the degree of uncertainty in flow depth estimates as well as to report a confidence level for the discharge estimations.

STUDY SITE

The Arroyo Cabrera (40° 24′N; 4° 39′W) is a fluvio-torrential watershed located on the northern slopes of the Sierra del Valle (Spanish Central System, Tagus Basin; Figure 1A). The catchment has an area of 15·75 km^2 and is formed by the confluence of several streams. The main channel has a length of ∼5500 m and presents an altitudinal range of ∼1230 m. The stream is characterized by high torrential activity owing to persistent and heavy rainstorms that are usually taking place in winter. These events result in abundant surface runoff, mobilization of sediments, and subsequent flash floods. At the study site, a hydrologic gauge network is operational since 2004. So far, the largest event recorded had a peak discharge of 20·7 m^3 s^{-1} resulting from a storm with a maximum rainfall intensity of 114·0 mm h^{-1} on 18 October 2004. Dendrogeomorphic data point to the presence of other events, such as those occurred recently in the winters of 1989/90 and 1997/98 (Ballesteros *et al*., 2010a), their magnitude remains, however, unknown.

The flash flood analysed in this paper took place on 17 December 1997 and was particularly severe. It resulted in abundant damage in the riparian vegetation

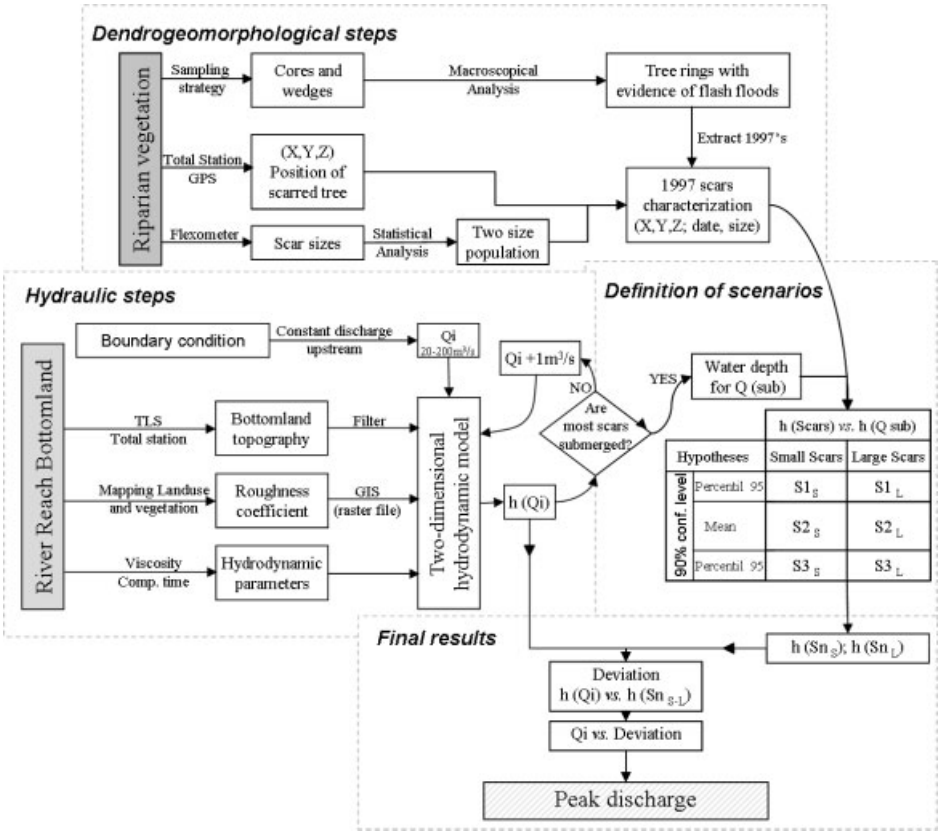

Figure 2. Methodological diagram used for palaeoflood discharge reconstruction. (Q_i = maximum peak discharge value; $h(Q_i)$ = water surface as a function of the maximum peak discharge; Q_{sub} = minimum peak discharge for which all scar are submerged; and Sn_{L-S} = impact depth scenario for the case of large scar (Sn_L) and small scar (Sn_S), respectively)

(mainly *Fraxinus angustifolia* Vhal., *Alnus glutinosa* (L.) Gaertn. and *Populus ssp*.) and largely redefined the stream architecture (Ballesteros *et al*., 2010b).

The assessment of peak discharge was realized in a reach located in the lower part of the catchment, with a length of 500 m and an average slope of 0·231 m/m (Figure 1B). This reach was chosen for its stable bedrock channel, ensuring that channel geometry did not change significantly during the flood analysed. Moreover, the reach is characterized by a high density of trees with PSI stemming from the impact of debris transported during the flash floods (Figure 1C).

METHODOLOGY

The methodology used to estimate the peak discharge of the 1997 event is an integration of (i) dendrogeomorphic techniques used to obtain observation points and to define hypothetical scenarios as well as (ii) hydraulic and topographic approaches to gather simulated water surface values. The different working steps used in this study are given in Figure 2.

Sampling and dating of scars on riparian trees

A sampling strategy has been designed to analyse and check that all PSI observed on the tree trunks of riparian vegetation stem from the 1997 flash flood. A total of 23 trees with scars orientated according to the flow direction were considered. Trees with scars located elsewhere on the stem or scars with doubtful geometry (i.e. unusually large or elongated scars) were avoided as they could have been generated through falling neighbouring trees. In trunks with several scars at different heights, the uppermost point of the highest scar was considered for the estimation of peak discharge.

Wedges of the overgrowing callus pad of wounded trees were taken with a handsaw and transported to the laboratory for dating. Additional information was obtained including scar size, tree diameter at breast height, as well as sketches and a description of the geomorphic position of the tree.

At the laboratory, all samples were air dried, sanded, and polished with sandpaper (up to 400 grit) to facilitate recognition of tree rings. Next, samples were scanned to conserve original images with high resolution. Tree-ring series of all samples were subsequently counted using a digital LINTAB positioning table connected to a stereomicroscope and TSAP 4·63 software (Rinntech, 2008; Stoffel and Bollschweiler, 2008). Wounds were located in the tree-ring record and events were dated with sub-annual resolution (Yanosky and Jarrett, 2002; Stoffel *et al*., 2008; Zielonka *et al*., 2008).

Topographical data acquisition

The terrestrial laser scanner TLS-CALLIDUS CP 3200 (Shan and Toth, 2008) was used for the acquisition of

topographic data along the 500-m reach analysed in this study. This technology allows to record millions of points over a surrounding scene or an object's x, y, and z information. Data are then displayed as a 'point cloud' which can be viewed, measured, and navigated as a 3D model. The main characteristics of the TLS used are (i) its maximum scope of 32 m, (ii) a precision of 5 mm on average, and (iii) a speed of sweep of 1750 points s^{-1}.

Because of the extension of the suited area together with the highly irregular reach topography and dense vegetation, it was necessary to use successive topographic stations to complete the scan of the whole model. On the other hand, a total station (TS) survey was used to acquire maximum scar heights and tree positions, as well as to complete the bathymetry in the main channel because TLS cannot characterize topography below water.

After the acquisition of topography, all data were registered and filtered to eliminate possible interferences, resulting in a filtered database with ~500 000 points (90 points m^{-2}) which were then used to generate a mesh as the main input to the hydraulic model.

Hydraulic model

The flow model used was the 2D hydrodynamic modular model MIKE 21 developed by the Danish Hydraulic Institute (DHI, 2008). This model operates with a numerical scheme of finite differences allowing to obtain real results in supercritical, subcritical, or mixed stationary regimes over different meshes (i.e. single, multiple, curvilinear, or flexible meshes). For the computation of the 2D approach as well as for the description of flow and water depth variations, the model uses 'alternating direction implicit' techniques which solve the conservation of mass momentum integrated over the vertical (DHI, 2008). Boundary conditions can be included as Q(t) (i.e. constant or variable peak discharge) or H(t) (i.e. constant or variable water stage). The roughness coefficient is included as a constant value or as a roughness grid file using either Manning's n or Chezy's C-values. The hydrodynamic model reports results on water depth, velocity as well as bed shear stress in x- and y-directions, therefore allowing for immediate results on stream power per unity area as

$$P = V\sqrt{\tau_x^2 + \tau_y^2} \tag{1}$$

where τ_x and τ_y are the bed shear stresses in the x- and y-directions, respectively; and V being the flow velocity.

In our flow model, topography was incorporated as a single mesh (pixel size 35 cm) through the Mike Zero application (DHI, 2008). Initial conditions were included as a constant discharge upstream in the range of 20–200 $m^3\ s^{-1}$ which allowed comparison of a given simulation with existing PSI. The roughness coefficient was implemented into the model as a grid file based on Manning's values ($m^{1/2}\ s^{-1}$). To this end, homogeneous patches were mapped in the field and assigned Manning's values taking into account the nature of the main channel and the associated floodplains (Aldridge and Garrett, 1973). In total, nine roughness units were identified between the main channel and the vegetated banks. Units include stable bedrock (values between 0·02 and 0·028 $m^{1/2}\ s^{-1}$), patches with big boulders (0·09 $m^{1/2}\ s^{-1}$), main channel (0·083 $m^{1/2}\ s^{-1}$), vegetated banks (between 0·11 and 0·15 $m^{1/2}\ s^{-1}$), and non-vegetated banks (0·03 $m^{1/2}\ s^{-1}$). The eddy viscosity was assessed at 0·0045 $m^2\ s^{-1}$ and therefore represents the maximum eddy viscosity value reported by Yoon and Kang (2005) for profiles near the bed and different sediment loads. Based on the above values, different simulation runs were carried out using different computational time ranges and time steps until the model was stable. The computational time used in our study was around 7 h with time steps of 0·015 s.

Palaeoflood discharge estimation

In order to produce more robust palaeoflood discharge estimations, we considered three different hypothetical water stage scenarios according to the size and height of scars observed in trees at the study reach.

Scenarios have been based on the statistical distribution of observed deviations (in %) between scar heights measured in the field and modeled water depths where all of these scars were fully submerged (Q_{sub}). This comparison has been performed for all scars simultaneously so as to minimize the overall error. Considering a bilateral confidence level of 90%, maximum (S_{max}) and minimum (S_{min}) scenarios were defined by the 5th and 95th percentile of the statistic distribution of observed deviations, respectively. On the other hand, the medium scenario (S_{med}) was defined as

$$\mu = E(x) = \int_{-\infty}^{\infty} x.f(x).\ \mathrm{d}x \tag{2}$$

where $f(x)$ represent the density function of the distribution obtained.

As a result of the gradation of scar sizes observed on trees impacted by flash floods, the above scenarios have been considered for two different populations of scars, i.e. large and small scars, being differentiated by means of a non-parametric statistical test (Sprent and Smeeton, 2001).

Peak discharge of the analysed palaeoflood event was then estimated using the step-backwater method (O'Connor and Webb, 1988; Benito *et al.*, 2003), which consists of a calculation of the water stage from peak discharge input in the model and a better fitting between the PSI identified and water surface elevation (Webb and Jarrett, 2002). For each scenario, we searched for those peak discharges that minimized the expression

$$\text{Deviation} = D_S \times \frac{n_S}{N_t} + D_L \times \frac{n_L}{N_t};$$

with

$$D_{S-L} = \frac{\sum_i^n (H_m \times 100)/H_e}{n}; \tag{3}$$

where D_{S-L} is the deviation rate for both small (S) and large (L) scar sizes; n_S and n_L are the number of S and L scars, respectively; N_t the total number of scars considered; H_m the averaged water stage evaluated at 1 m^2 around the tree; and H_e the expected water height, defined by the expression

$$H_e = h_{PSI} + h_{[Qi]} \times (1 - S_k); \quad (4)$$

with h_{PSI} being the maximum scar height (Gottesfeld, 1996; Yanosky and Jarrett, 2002); and the product $h_{[Qi]} \times (1 - S_k)$ the hypothetical impact depth for the scenario S_k and the water depth h obtained with the hydraulic model for discharge Q_i.

RESULTS

Tree scars and dendrogeomorphic dating

A total of 23 trees within the study reach showed visible scars resulting from the impact of sediment and woody material transported during flash floods. A majority of scars (18 trees) were identified in *Alnus glutinosa* (L.) Gaertn. and five in *Fraxinus angustifolia* Vahl. In addition, five trees showed a scar-size gradation. Figure 3 shows the position of trees with PSI and their heights with respect to the longitudinal channel profile. Most scars were found in the lower part of the study reach where the slope is more gently; but this result also reflects the fact that trees have greater difficulties to colonize the steeper segments of the bedrock reach.

Dendrogeomorphic analysis also reveals that all scars were caused by the 1997 flash flood. An overview on the different PSI used in this study (i.e. geographical location of trees, scar size, and event dating) is provided in Table I.

Definition of flash flood scenarios for peak discharge estimation

Two scar size populations were differentiated by means of a non-parametric W test (p-value <0·001, 95% confidence interval). Wounds with visible scarred areas <800 cm^2 were defined as small scars. In contrast, scars were defined large when the area visibly damaged during the 1997 flash flood was ≥800 cm^2. In a subsequent step, peak discharge Q_{sub} of the 1997 event was defined as 145 $m^3\ s^{-1}$ (Figure 4). This value represents the minimum peak discharge for which all scars are submerged and therefore defines a reference level for PSI to estimate the hypothetical depth of the flow.

Results of the deviation between the maximum scar heights for both small and large scars and the water table for Q_{sub} are provided in Table II. They provide a minimum p-value of the three normality tests (χ^2-goodness of fit; Shapiro–Wilks' W test; Z-asymmetry statistics) of 0·4057 which allowed in turn an assessment

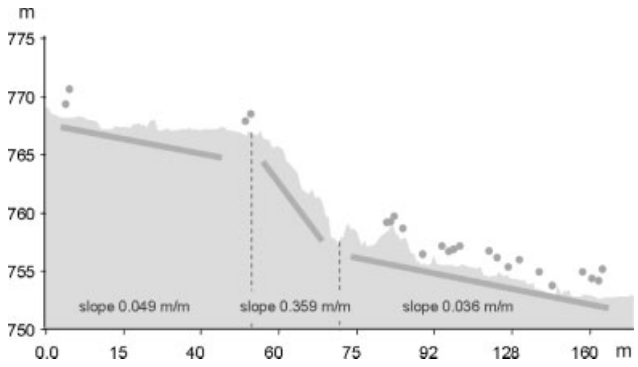

Figure 3. Scar-height distribution along the study reach profile

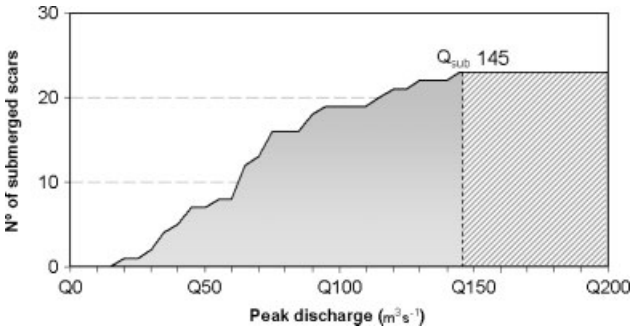

Figure 4. Definition of peak discharge corresponding to Q_{sub}

Table I. Description of PSI (i.e. scar on trees) used in the study

Tree code	X_{UTM}	Y_{UTM}	Scar size (cm^2)	Tree code	X_{UTM}	Y_{UTM}	Scar size (cm^2)
1	359 174	4 474 281	130	13	359 192	4 474 363	380*
2	359 173	4 474 282	250	14	359 201	4 474 371	1550
3	359 199	4 474 303	160*	15	359 199	4 474 374	1150
4	359 210	4 474 297	848	16	359 198	4 474 354	1050
5	359 220	4 474 335	2650	17	359 195	4 474 380	150
6	359 222	4 474 334	1620	18	359 225	4 474 343	640
7	359 223	4 474 335	1056	19	359 191	4 474 402	750
8	359 223	4 474 338	558	20	359 178	4 474 404	525
9	359 224	4 474 345	1044	21	359 180	4 474 405	100
10	359 217	4 474 352	210*	22	359 177	4 474 407	3150
11	359 216	4 474 352	540*	23	359 188	4 474 413	1369
12	359 215	4 474 352	800*				

* Samples with scar size gradation.

Table II. Comparison between the water surface elevation (WSE) obtained with the hydraulic model for Q_{sub} and maximum scar heights

Small scars					Large scars				
Number of trees	WSE Q_{sub}	Maximum scar height	Δ (m)	Δ (%)	Number of trees	WSE Q_{sub}	Maximum scar height	Δ (m)	Δ (%)
1	3·05	1·76	1·29	57·6	4	2·16	0·93	1·23	43·0
2	3·60	2·50	1·10	69·3	5	1·37	0·77	0·60	56·0
3	2·14	1·60	0·54	74·7	6	2·46	0·60	1·86	24·3
8	1·13	0·87	0·66	41·4	7	2·24	0·33	1·91	14·6
10	3·30	1·40	1·90	42·3	9	1·98	0·88	1·10	44·3
11	3·79	1·50	2·29	39·5	12	3·85	1·90	1·95	49·3
13	4·27	2·20	2·07	51·4	14	2·63	2·20	0·43	83·3
17	2·40	2·15	0·25	89·6	15	2·28	1·60	0·68	69·9
18	2·97	1·60	1·37	53·8	16	1·27	1·10	0·17	86·5
19	3·19	1·85	1·34	57·9	22	3·99	0·90	3·09	22·5
20	4·17	1·30	2·87	31·1	23	4·43	2·40	2·03	54·1
21	2·22	2·22	0	99·6					
Normally tested		Minimum *p*-value (asymmetry statistic)		0·405	Minimum *p*-value (Shapiro–Wilks)				0·679

(95% confidence level) of deviation from a normal distribution $N \sim (\mu, \sigma)$.

In the case of small scars (Figure 5A), deviation is described as $N \sim (59{\cdot}02, 20{\cdot}81)$. Considering a confidence interval of 90%, the minimum scenario (S_{min}) is described for the 95th percentile corresponding to a deviation of 99·6%; whereas the maximum scenario (S_{max}) is defined by the 5th percentile corresponding to a deviation of 31·1%. The medium scenario (S_{med}) is defined by the expectation value (i.e. the mathematical expectation) and corresponds to 59·0%. In the case of large scars (Figure 5B), deviation is described as $N \sim (49{\cdot}85, 23{\cdot}75)$, defining a minimum scenario (S_{min}) with a deviation of 86·5%, a maximum scenario (S_{max}) with a deviation value 14·6%, and a medium scenario with a deviation of 49·9%.

Figure 6 shows the deviation rate between the expected heights for the three scenarios defined and the modeled results of peak discharge ranging from 20 to 200 $m^3\ s^{-1}$. As can also be seen from Figure 6, peak discharge values correspond with the minimum deviation rate for S_{min} at 67 $m^3\ s^{-1}$ (deviation = 1·9%; variance = 0·39 m); whereas for S_{med}, the smallest absolute deviation rate is obtained with a peak discharge of 79 $m^3\ s^{-1}$ (deviation = 1·2%; variance = 0·39 m), and at 95 $m^3\ s^{-1}$ (deviation = 1·0%; variance = 0·50 m) for S_{max}. Based on this data, peak discharge of the 1997 flash-flood event at Venero Claro is estimated to $79 \pm 14{\cdot}4\ m^3\ s^{-1}$ with an average deviation between expected heights and modeled water surface of 1·15%.

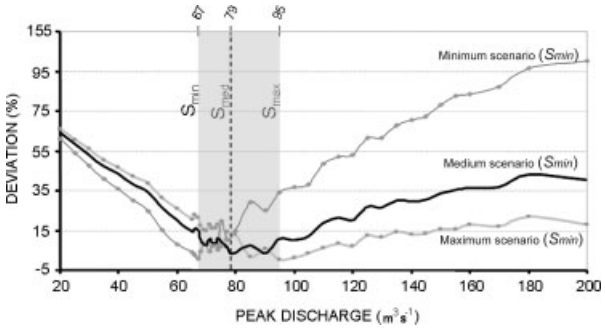

Figure 6. Definition of peak discharge of the 1997 flash flood event based on minimum deviation rates for each of the scenarios (S_{min}, S_{med}, and S_{max}). (For details see text)

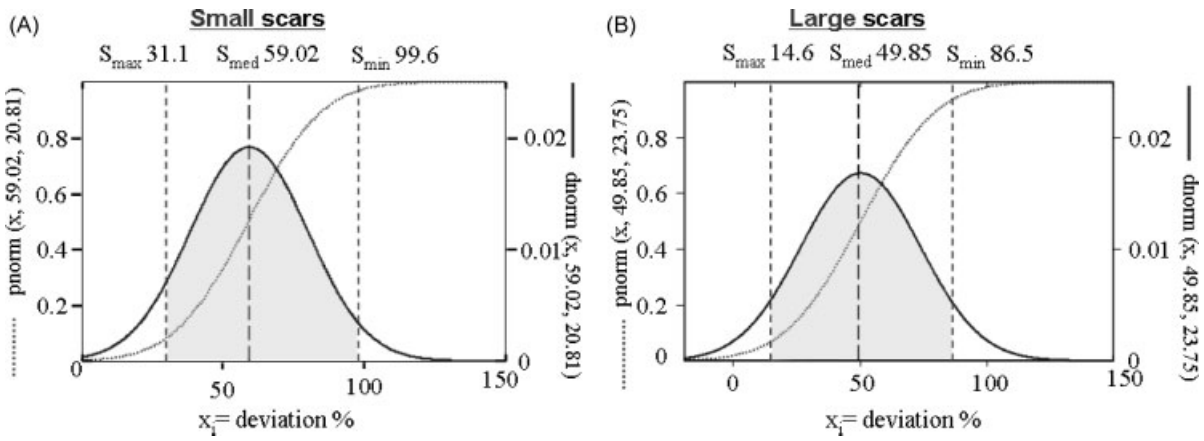

Figure 5. Density and distribution functions of deviation between scar height and water tables of Q_{sub} for both small (A) and large scars (B). Statistical analyses were carried out with the MATHCAD software (http://www.ptc.com/products/mathcad/)

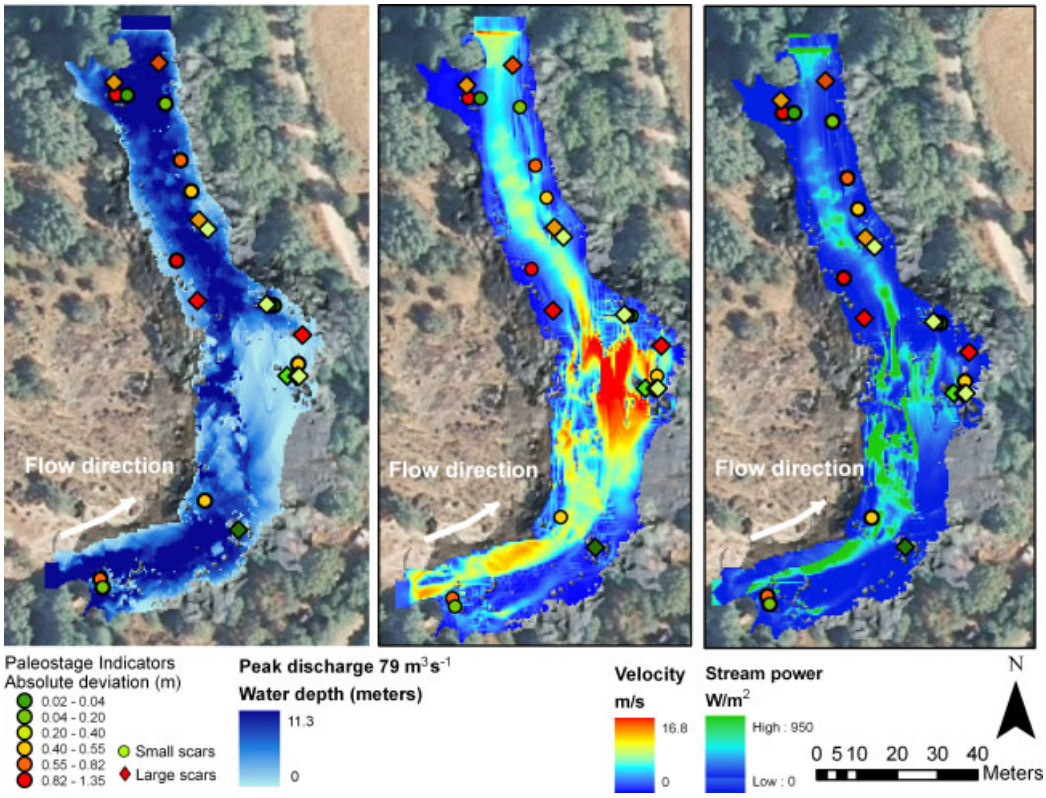

Figure 7. Absolute deviation (in m) of PSI as observed on tree trunks and their relation with water depth, flow velocity, and stream power for the estimated 1997 event

Relation between scar height and water depth, flow velocity and power stream

Figure 7 illustrates the relationship between the deviation rates obtained and scar sizes with hydraulic characteristics such as water depth, flow velocity, and stream power for the estimated peak discharge. Noteworthy, scar sizes showed trends in their pattern of distribution. In 65% of the cases, large scars were identified in trees located in more upstream positions as compared to trees with smaller scars.

Deviation between the water table and scar heights was between $-0{\cdot}88$ and $+1{\cdot}35$ m, resulting in an average deviation of $-0{\cdot}09$ m ($\sigma = 0{\cdot}53$). Small deviations ($<0{\cdot}2$ m) were observed in 52% of the cases. Most of these trees grow at sites which are quite exposed to the flow, i.e. especially in the reach with the steepest slopes and unruffled bedrock where specific kinetic energy tends to be higher as well.

The maximum simulated stream power was close to 950 W m^{-2} and modeled in the central part of the channel where water depth and flow velocity are the highest. In the case of scar formation in trees, stream power values are expected to be much lower, possibly <10 W m^{-2}. However, stream power data did not reveal a significant relation with deviation rates or scar sizes.

DISCUSSION

In this paper, we have presented a combined approach using different flash flood stage scenarios based on PSIs on trees and 2D hydraulic models to estimate peak discharge of a palaeoflood in an ungauged mountain torrent in the Spanish Central System. Modeling was performed on a highly accurate topography obtained through a detailed survey with a TLS of the study reach.

The methodology presented here represents a novel approach for research focused on palaeodischarge estimations and one of the first attempts to use scars on trees for magnitude reconstruction of flood events and in more than 1D (see Egginton and Day, 1977; Yanosky and Jarrett, 2002). In addition, this study was also the first to combine scars on trees with accurate 2D hydraulic models, which certainly helps to improve the understanding on how scars on trees can be used as PSI in palaeohydrology.

The main contribution of this study was the definition of different scenarios based on scar size and the relationship between peak discharges needed to submerge all PSI (Q_{sub}). This approach has also allowed quantification of uncertainty associated with peak discharge estimates in high gradient streams based on tree scars. Despite the good agreement of field and model results, some methodological issues related to the hydraulic model as well as the complexity of flash-flood processes studied and their relationship with scar generation on trees merit further discussion.

In the present case, the simulation of peak discharge was carried out with a 2D hydraulic model running on an accurate topography obtained with a TLS, which proved to be especially useful for flow estimation over complex

surfaces (Denlinger *et al*., 2002; Baker, 2008). Although roughness coefficients could not be calibrated along the main channel due to lacking data, the uniformity of bedrock present in the study reach greatly helped the assignment of Manning's values (Kidson *et al*., 2006) as well as the elimination of inaccuracies due to topographic changes resulting from process dynamics (Webb and Jarrett, 2002).

The approach presented is also consistent with the classical debris transport theory (Aristide *et al*., 2006; Mintegui *et al*., 2006). At Venero Claro, a torrent characterized by a steep gradient, large scars have been observed at lower heights as compared to small scars, which interpreted the result of the gradation in size of debris transported. In our case, debris mainly consisted of boulders and woody debris: it was transported by the flash flood through saltation and bed load (Bodoque *et al*., 2006). Webb and Jarret (2002) suggest that woody debris can be transported partially submerged, which could explain the dispersion on deviation. Another reason for scars located above the actual water stage level could be caused by the deposition of woody material around stems during the flash flood and a subsequent localized super-elevation of the flow (Darby, 1999; Carling *et al*., 2002). Last but not the least, it is also possible that elongated scars were generated by a longitudinal propagation of cambium tissue and fiber damage and could therefore have resulted in upper limits of scars above the actual flow level. On the other hand, it is also possible that our approach underestimates peak flow in case when scars would be formed before or after peak flow at the study reach. However, based on our observations, we agree with Gottesfeld (1996) that flood scar formation is most likely to occur during peak stages. A comparison of PSI with HWMs data may help to answer the above questions. In the present case, however, such a comparison was not possible as evidence of HWM (Williams and Costa, 1988; Jarrett and England, 2002) is no longer visible at the study site.

The approach presented in this study is based on the deviation between maximum scar heights and data from hydraulic model runs. The minimum peak discharge needed to submerge all PSI (Q_{sub}) was defined at 145 $m^3\ s^{-1}$. Scars on trees are used here as PSI and therefore it indicates the flood level that has been exceeded during a given flood (Baker, 2008). Rather than using a single value for the definition of this peak discharge reference (Q_{sub}), we hypothesize that flood marks may eventually occur above or below the flood level. This hypothesis is in agreement with results obtained by Gottesfeld (1996) or Yanosky and Jarrett (2002), who studied the relationship between scar distributions on trees and adjacent HWM.

Therefore, the comparison of modeled hydraulic parameters with scar generation illustrates that there is no relationship between stream power and the deviation obtained; this is probably due to the fact that affected trees were placed on banks where stream power was much lower (<10 W m^{-2}). In this sense, the geomorphic position of trees appeared as the main factor explaining this deviation. Better fits (<0·2 m) were found for (i) trees in exposed positions with respect to the flow direction, (ii) locations with higher flow velocities and for (iii) lower water depths. In contrast to Gottesfeld (1996), we cannot see any relationship between lateral tree position and deviation, as the incisions present at the study reach prevented tree growth in lateral positions.

Our results also show a deviation between scar height and water table between −0·88 and +1·35 m. Twelve scars (52% of cases) are within an acceptable deviation of ±0·2 m and the entire scar population defines an average deviation of $-0{\cdot}09 \pm 0{\cdot}53$ m. These values are comparable to those obtained by Yanosky and Jarrett (2002) in a high-gradient stream where observed deviations between scar heights and HWM ranged from −0·6 to 1·5 m. However, similar to our case, more than half of their scars were within ±0·2 m as well. In contrast, our deviation results are more important than those presented by Gottesfeld (1996) for torrents with lower stream gradients in British Columbia (i.e. $0{\cdot}196 \pm 0{\cdot}03$ m).

Based on the above considerations, a peak discharge was estimated for the 1997 event at Venero Claro and assessed at $79 \pm 14\ m^3 s^{-1}$, with an uncertainty in the rank of 18·8%. Following Jarrett and England (2002) this value is within the acceptable limits of palaeoflood discharge estimates based on mean PSI. Compared to the flow data series available at Venero Claro, the reconstructed peak discharge of the 1997 flash flood suggests an event almost four times larger than the biggest event on record as the instrumentation of the torrent in 2004 (i.e. 20·3 $m^3\ s^{-1}$; Ballesteros *et al*., 2010a), and is assigned a yearly exceedance probability of 0·02 according to CEDEX (2009). Despite of the high exceedance probability associated to our results, field recognition allowed to report a heavy flood impact in the river corridor (Díez, 2001), especially in the upper half of the basin. In agreement with Montgomery and Buffington (1997) or Rickenmann and Koschni (2010), we believe that this discrepancy between the peak discharge estimated at the study reach and field observations in the upper half of the basin are closely related to the evolution of hydrologic processes between the headwaters (i.e. diffusion to debris-flow dominated processes) and the lower parts of the basin (i.e. predominantly fluvial processes). On the other hand, the existence of a small reservoir and several small bridges upstream of the study site could also have helped to reduce peak flow at the study reach.

CONCLUSIONS

In this paper, we have shown that peak discharge of palaeofloods in ungauged mountain catchments can be realistically estimated by coupling dendrogeomorphic techniques with 2D hydraulic models. The approach presented is based on the definition of different scenarios and has allowed to obtain results with acceptable uncertainly,

thus resulting in valuable data which will ultimately help to further improve our understanding of flash flood processes in mountain regions of the Mediterranean area.

This paper has also made a first step towards the use of scar-size gradation in palaeoflood discharge estimations and on how they can be used for the evaluation of hypothetical impact heights. Although, more research is needed to relate, e.g. scar generation with HWM, we were able to illustrate that the geomorphic position of trees plays a pivotal role for the understanding of deviation rates obtained and proved to be one of the key factors to be taken into account in sampling strategies for flood studies based on tree-ring series. Future comparisons between scar height and data from debris lines, video evidence of floodwater heights, as well as the transport characteristics of woody debris will ultimately help to clarify some of the issues presented here.

ACKNOWLEDGEMENTS

This paper was funded in part by the CICYT, the DendroAvenidas project (number CGL2007-62063 of the Spanish Ministry of Science and Innovation) and the Instituto Geológico y Minero de España (IGME). The authors acknowledge the valuable feedback of the anonymous reviewers and colleagues Virginia Ruiz, Teresa Herrero, and Hector Aguilera, as well as the kind collaboration of the Environment Department of Ávila (Castilla-Leon), in particular forester J. L. Galán.

REFERENCES

Aldridge BN, Garrett JM. 1973. Roughness coefficients for stream channels in Arizona. U.S. Geological Survey. Open-File Report 73-0003; 87.

Alestalo J. 1971. Dendrochronological interpretation of geomorphic processes. *Fennia* **105**: 1–140.

Aristide M, Mao L, Comiti F. 2006. When does bedload transport begin in steep boulder-bed streams? *Hydrological Processes* **20**(16): 3517–3533.

Baker VR. 2008. Paleoflood hydrology: origin, progress, prospects. *Geomorphology* **101**: 1–13.

Baker VR, Webb RH, House PK. 2002. The scientific and societal value of paleoflood hydrology. In *Ancient Floods, Modern Hazards: Principles and Applications of Paleoflood Hydrology. Water Science and Application*, Vol. 5, House PK, Webb RH, Baker VR, Levish DR (eds). American Geophysical Union: Washington, DC; 1–19.

Ballesteros JA, Stoffel M, Bodoque JM, Bollschweiler M, Hitz O, Díez-Herrero A. 2010a. Changes in wood anatomy in tree rings of *Pinus pinaster* Ait. following wounding by flash floods. *Tree Ring Bulletin* **66**(2): 93–103.

Ballesteros JA, Stoffel M, Bollschweiler M, Bodoque JM, Díez-Herrero A. 2010b. Flash-flood impacts cause changes in wood anatomy of *Alnus glutinosa, Fraxinus angustifolia* and *Quercus pyrenaica*. *Tree Physiology* **30**(6): 773–781.

Benito G, Rico M, Sánchez-Moya Y, Sopeña A, Thorndycraft VR, Barriendos M. 2009. Assessing the impact of late Holocene climatic variability and human impact on flood hydrology: the Guadalentin case study (SE Spain). *Global and Planetary Sciences* **70**(1–4): 53–63.

Benito G, Thorndycraft VR (eds). 2004. *Systematic, Palaeoflood and Historical Data for the Improvement of Flood Risk Estimation, Methodological Guidelines*. CSIC: Madrid; 115.

Benito G, Díez-Herrero A, Fernández de Villalata M. 2003. Magnitude and frequency of flooding in the Tagus basin (Central Spain) over the last millennium. *Climatic Change* **58**: 171–192.

Bodoque JM, Díez A, De Pedraza J, Martín JF, Olivera JF. 2006. Estimación de la carga sólida en avenidas de derrubios mediante modelos geomecánicos, hidrológicos e hidráulicos combinados: Venero Claro (Ávila). In *Geomorfología y territorio*, Pérez A, López J (eds). Universidad de Santiago de Compostela; Santiago de Compostela; 483–495.

Borga M, Boscolo P, Zanon F, Sangati M. 2007. Hydrometeorological analysis of the August 29, 2003 flash flood in the eastern Italian Alps. *Journal of Hydrometeorology* **8**(5): 1049–1067.

Carling PA, Hoffman M, Blatter AS. 2002. Initial motion of boulders in bedrock channel. In *Ancient Floods, Modern Hazards: Principles and Applications of Paleoflood Hydrology.Water Science and Application*, vol. 5, House PK, Webb RH, Baker VR, Levish DR (eds). American Geophysical Union: Washington, DC; 147–160.

CEDEX. 2009. *Mapa de Caudales Máximos en la Cuenca del Tajo*. Caumax versión 1.1. CD.

Chiang YM, Chang FJ. 2009. Integrating hydrometeorological information for rainfall-runoff modelling by artificial neural networks. *Hydrological Processes* **23**(11): 1650–1659.

Chow VT. 1959. *Open-channel Hydraulics*. McGraw-Hill: New York; 197.

Cook JL. 1987. Quantifying peak discharges for historical floods. *Journal of Hydrology* **96**: 29–40.

Corriell F. 2002. *Reconstruction of a paleoflood chronology for the middlebury river gorge using tree scars as flood stage indicators*, Unpublished senior thesis, Middlebury College. Department of Geology, Middlebury; 45.

Darby S. 1999. Effect of riparian vegetation on flow resistence and flood potential. *Journal of Hydraulic Engineering* **125**(5): 443–454.

Denlinger RP, O'Connell DRH, House PK. 2002. Robust determination of stage and discharge: an example from an extreme flood on the Verde River, Arizona. In *Ancient Floods, Modern Hazards: Principles and Applications of Paleoflood Hydrology. Water Science and Application*, vol. 5, House PK, Webb RH, Baker VR, Levish DR (eds). American Geophysical Union: Washington, DC; 127–146.

DHI. 2008. *MIKE 21 Flow Model. Hydrodinamic Module*. Scientific Documentation. DHI; 60.

Díez A. 2001. *Geomorfología e Hidrología fluvial del río Alberche. Modelos y SIG para la gestión de riberas*, PhD thesis, Universidad Complutense de Madrid, Madrid, 610. (http://www.ucm.es/BUCM/tesis/geo/ucm-t25361.pdf).

Egginton PA, Day TJ. 1977. Dendrochronologic investigation of high-water events along Hodgson Creek, District of Mackenzie. *Geological Survey of Canada* **77-1A**: 381–384.

Enzel Y, Ely LL, House PK, Baker VR, Webb RH. 1993. Palaeoflood evidence for a natural upper bound to flood magnitudes in the Colorado River basin. *Water Resources Research* **29**: 2287–2297.

Gaume E, Bain V, Bernardara P, Newinger O, Barbuc M, Bateman A, Blaskovicova L, Blöschl G, Borga M, Dumitrescu A, Daliakopoulos I, Garcia J, Irimescu A, Kohnova S, Koutroulis A, Marchi L, Matreata S, Medina V, Preciso E, Sempere-Torres D, Stancalie G, Szolgay Jan, Tsanis I, Velasco D, Viglione A. 2009. A collation of data on European flash floods. *Journal of Hydrology* **367**(1–2): 70–78.

Gottesfeld AS. 1996. British Columbia flood scars: maximum flood-stage indicator. *Geomorphology* **14**: 319–325.

Gottesfeld AS, Gottesfeld LMJ. 1990. Floodplain dynamics of a wandering river, dendrochronology of the Morice River, British Columbia, Canada. *Geomorphology* **3**: 159–179.

Harrison SS, Reid JR. 1967. A flood-frequency graph based on tree-scar data. *Proceedings of the North Dakota Academy of Science* **21**: 23–33.

Jarrett RD. 1990. Hydrologic and hydraulic research in mountain rivers. *Water Resources Bulletin* **26**(3): 419–429.

Jarrett RD, England JF Jr. 2002. Reliability of paleostage indicators for paleoflood studies. In *Ancient Floods, Modern Hazards: Principles and Applications of Paleoflood Hydrology. Water Science and Application*, vol. 5, House PK, Webb RH, Baker VR, Levish DR (eds). American Geophysical Union: Washington, DC; 91–109.

Kidson RL, Richards KS, Carling PA. 2006. Hydraulic model calibration for extreme floods in bedrock-confined channels: case study from northern Thailand. *Hydrological Processes* **20**(2): 329–344.

Livingston JM, Smth DG, Froese DG, Hugenholtz CH. 2009. Floodplain stratigraphy of the ice jam dominated middle Yukon River: a new approach to long-term flood frequency. *Hydrological Processes* **23**(3): 357–371.

Merz B, Elmer F, Thieken AH. 2009. Significance of "high probability/low damage" versus "low probability/high damage" flood events. *Natural Hazards and Earth System Sciences* **9**: 1033–1046.

Mintegui JA, Aristide M, Robredo JC, Mao L. 2006. *Movilización versus estabilización de los sedimentos en los cursos sometidos a la dinámica torrencial. Análisis de dos casos: el río Cordón (Alpes*

Dolomitas, Italia) y el arroyo del Partido (Parque Nacional de Doñana, España). Naturaleza y Parques Nacionales. Technical series, Organismo Autónomo de Parques Nacionales, Ministerio de Medio Ambiente, Madrid.

Mintegui JA, Robredo JC. 2008. *Estrategias para el Control de los Fenómenos Torrenciales y la Ordenacion Sustentable de las Aguas, Suelos y Bosques de las Cuencas de Montaña.* UNESCO. Documentos Técnicos del PHI-LAC N°13. 162. Published on line (http://www.unesco.org.uy/phi).

Montgomery DR, Buffington JM. 1997. Channel-reach morphology in mountain drainage basins. *Geological Society of America Bulletin* **109**: 596–611.

O'Connor JE, Webb RH. 1988. Hydraulic modelling for paleoflood analysis. In *Flood Geomorphology*, Baker VC, Kochel RC, Patton PC (eds). Jhon Wiley & Sons, Inc.: New York; 393–402.

Payrastre O, Gaume E, Andrieu H. 2005. Use of historical data to assess the occurrence of floods in small watersheds in the French Mediterranean area. *Advances in Geosciences* **2**: 313–320.

Rickenmann D, Koschni A. 2010. Sediment loads due to fluvial transport and debris flows during the 2005 flood events in Switzerland. *Hydrological Processes* **24**: 993–1007 DOI: 10.1002/hyp.7536.

Rinntech. 2008. *LINTAB. Precision ring by ring*. Published on line http://www.rinntech.com/Products/Lintab.htm..

Ruiz-Villanueva V, Díez-Herrero A, Stoffel M, Bollschweiler M, Bodoque JM, Ballesteros JA. 2010. Dendrogeomorphic analysis of flash floods in a small ungauged mountain catchment (Central Spain). *Geomorphology* **118**: 383–392.

Scheuren J-M, le Polain de Waroux O, Below R, Guha-Sapir D. 2008. Annual Disaster Statistical Review: The Numbers and Trends 2007. Centre for Research on the Epidemiology of Disasters (CRED). Catholic University of Louvain (UCL): Brussels. Published on line http://www.emdat.be/.

Shan JC, Toth K (eds). 2008. *Topographic Laser Ranging and Scanning: Principles and Processing*. CRC Press/Taylor & Francis Group; 608.

Sprent P, Smeeton NC. 2001. *Applied Nonparamentric Statistical Methods*. Chapman & Hall/CRC: Boca Raton, FL, London, New York, Washington, DC.

St. George S, Nielsen E. 2003. Palaeoflood records for the Red River, Manitoba, Canada, derived from anatomical tree-ring signatures. *Holocene* **13**(4): 547–555.

Stoffel M. 2010. Magnitude-frequency relationships of debris flows—A case study based on field surveys and tree-ring records. *Geomorphology* **116**: 67–76.

Stoffel M, Bollschweiler M, Butler DR, Luckman BH. 2010. *Tree Rings and Natural Hazards: A State-of-the-art*. Springer: Heildelberg, Berlin, New York; 505.

Stoffel M, Conus D, Grichting MA, Lièvre I, Maître G. 2008. Unraveling the patterns of late Holocene debris-flow activity on a cone in the Swiss Alps: chronology, environment and implications for the future. *Global and Planetary Change* **60**: 222–234.

Webb RH, Jarrett RD. 2002. One-dimensional estimation techniques for discharges of paleofloods and historical floods. In *Ancient Floods, Modern Hazards: Principles and Applications of Paleoflood Hydrology: Water Science and Application*, vol. 5, House PK, Webb RH, Baker VR, Levish DR (eds). American Geophysical Union: Washington, DC; 111–126.

Williams GP, Costa JE. 1988. Geomorphic measurement after a flood. In *Flood Geomorphology*, Baker VC, Kochel RC, Patton PC (eds). Jhon Wiley & Sons, Inc.: New York; 65–77.

Yanosky TM, Jarrett RD. 2002. Dendrochronologic evidence for the requency and magnitud of palofloods. In *Ancient Floods, Modern Hazards: Principles and Applications of Paleoflood Hydrology: Water Science and Application*, vol. 5, House PK, Webb RH, Baker VR, Levish DR (eds). American Geophysical Union: Washington, DC; 77–89.

Yoon J-F, Kang S-K. 2005. A numerical model of sediment-laden turbulent flow in an open channel. *Canadian Journal of Civil Engineering* **32**: 233–240.

Zielonka T, Holeksa J, Ciapala S. 2008. A reconstruction of flood events using scarred tree in the Tatra Mountains, Poland. *Dendrochronologia* **26**: 173–183.

